Magnetoreflection Studies in Bismuth†*

Martin Maltz‡
Department of Electrical Engineering, and Center for Materials Science and Engineering, Massachusetts Institute of Technology, Cambridge, Massachussetts 02139

and

M. S. Dresselhaus‡
Department of Electrical Engineering, Center for Materials Science and Engineering, and Lincoln Laboratory, Massachusetts Institute of Technology Cambridge, Massachusetts 02139

(Received 19 February 1970)

Detailed magnetoreflection studies on the binary and bisectrix faces of bismuth are made to look for the fine structure predicted by the Baraff generalization of the Lax two-band model. This generalization is required to explain certain structure in the de Haas–van Alphen data. No fine structure is found experimentally in the magnetoreflection spectra for these optical faces. Magnetoreflection data were also taken for $\vec{H}$ in the trigonal direction to look for expected departures from the Lax model. No such departures were found. By assuming a particularly simple form for the Baraff Hamiltonian, it is possible to explain both the magnetoreflection and de Haas–van Alphen data, which had previously been thought to be inconsistent.

I. INTRODUCTION

The tightly coupled conduction and valence bands of bismuth (see Fig. 1) have been studied extensively by a number of experimental and theoretical techniques.[1] One particularly informative experiment has been the infrared magnetoreflection study of Brown, Mavroides, and Lax (BML).[2] In this experiment, resonances in the magnetoreflectivity were observed and identified with interband transitions between Landau levels in these strongly coupled valence and conduction bands. These data, which indicated that the bands had extremely nonparabolic dispersion relations, could be understood in terms of the coupled two-band model.[3-6] This band model assumes that the two coupled bands interact only with each other and results in a spectrum of nonuniformly spaced Landau levels which remain doubly degenerate even in the presence of spin-orbit interaction.

The magnetic energy levels for bismuth as given by the Lax two-band model[4,6] can be written as[7]

$$E^0_{b,j}(k_H) = \pm\left[\epsilon^2 + 2\epsilon(\beta^* H j + \hbar^2 k_H^2/2m_H)\right]^{1/2}, \tag{1}$$

where k_H is the wave vector along the magnetic field. These magnetic energy levels are labeled by the band index b and quantum number j. For $k_H = 0$, these levels depend only upon two parameters: the energy gap E_g and the cyclotron effective mass m_c^*. These parameters are related to quantities in Eq. (1) by

$$E_g = 2\epsilon \tag{2}$$

and

$$m_c^* = m_0\beta_0/\beta^*, \tag{3}$$

where m_0 is the free-electron mass, $\frac{1}{2}\beta_0$ is the magnitude of the Bohr magneton, $\beta_0 = |e|\hbar/m_0c$, and the quantity β^* is related to the effective-mass tensor $\vec{\vec{m}}^*$ by

$$\beta^* = \beta_0(\hat{h}\cdot\vec{\vec{m}}^*\cdot\hat{h})^{1/2}/\det\vec{\vec{m}}^*)^{1/2}, \tag{4}$$

where $\hat{h}$ is a unit vector in the direction of the magnetic field, and $\det\vec{\vec{m}}^*$ signifies the determinant of the matrix for the effective-mass tensor. The + and − signs in Eq. (1) denote, respectively, the conduction band ($b = +1$) and valence band ($b = -1$) of the coupled two-band model. The magnetic energy-level index j in Eq. (1) is related to the orbital and spin quantum numbers n and s by

$$j = n + \tfrac{1}{2} - s, \tag{5}$$

where $n = 0, 1, 2, \ldots$ and $s = \pm\frac{1}{2}$. The k_H dependence of the energy levels involves the longitudinal effective mass m_H,

$$m_H = \hat{h}\cdot\vec{\vec{m}}^*\cdot\hat{h}\ , \tag{6}$$

and assumes the simple form of Eq. (1). Of particular interest to the magnetoreflection experiment are the extrema in the magnetic energy levels which occur at $k_H = 0$ and are denoted in this paper by $E^0_{b,j}$ rather than the more cumbersome form $E^0_{b,j}(0)$. It is these levels $E^0_{b,j}$ of the two-band model that have been used by BML for the interpretation of the observed magnetoreflection spectrum.[2]

The magnetic energy-level structure of bismuth has also been extensively studied by experimental techniques which detect the passage of Landau levels through the Fermi surface [de Haas–van Alphen (dHvA),[8] de Haas-Shubnikov,[9] magnetothermal oscillations,[10] and ultrasonic magnetoabsorption[11] measurements]. These experiments, which we will

call dHvA-type studies, measure the magnetic field at which the Landau levels at $k_H = 0$ pass through the Fermi level. The fine structure observed in the dHvA studies clearly indicates that the Landau levels are not degenerate; the energy levels, instead of depending only upon the single quantum number j, do, in fact, depend upon both n and s of Eq. (5). That is, the effective g factor for the electrons does give rise to a spin splitting of the Landau levels. Baraff[12] assumed that this splitting was due to the small interaction of the tightly coupled valence and conduction bands with the other bands nearby and calculated the expected Landau-level energies to first order in perturbation theory. His results indicated that fine structure might be observable in the magnetoreflection spectrum in bismuth. Since the equipment of BML had been greatly improved in recent years,[13] we repeated their experiments in order to look for such fine structure. However, no fine structure is found in the present magnetoreflection study, indicating that the interaction of the tightly coupled bands with the bands nearby has a particularly simple form. The simplified equations, which explain both the splitting observed in the dHvA-type experiments and the absence of splitting in the resonances in the magnetoreflectivity, are presented in this paper.[14]

Perhaps even more important than these binary and bisectrix studies is the work carried out with $\vec{H}$ along the trigonal direction; this is so for several reasons. First of all, magnetoreflection oscillations due to interband transitions have not been previously observed with this sample orientation due to the very small amplitude of the resonances. Secondly, it has been known for some time that the Fermi surface for the electrons in bismuth consists of three ellipsoids which are centered at the L points in the Brillouin zone, and are greatly elongated along one of the principal axes (the heavy-mass axis). It has, therefore, been pointed out[5] that the two-band model may not provide an adequate description of the dispersion relation along the heavy-mass direction, since it is expected that in this direction the close-lying valence and conduction bands should not be tightly coupled at all. Moreover, the heavy-mass direction is nearly perpendicular to the trigonal axis (about 84° away), and, therefore, it is expected that any significant departures from the two-band model along the heavy-mass direction should lead to observable effects in the magnetoreflection data for $\vec{H}$ along

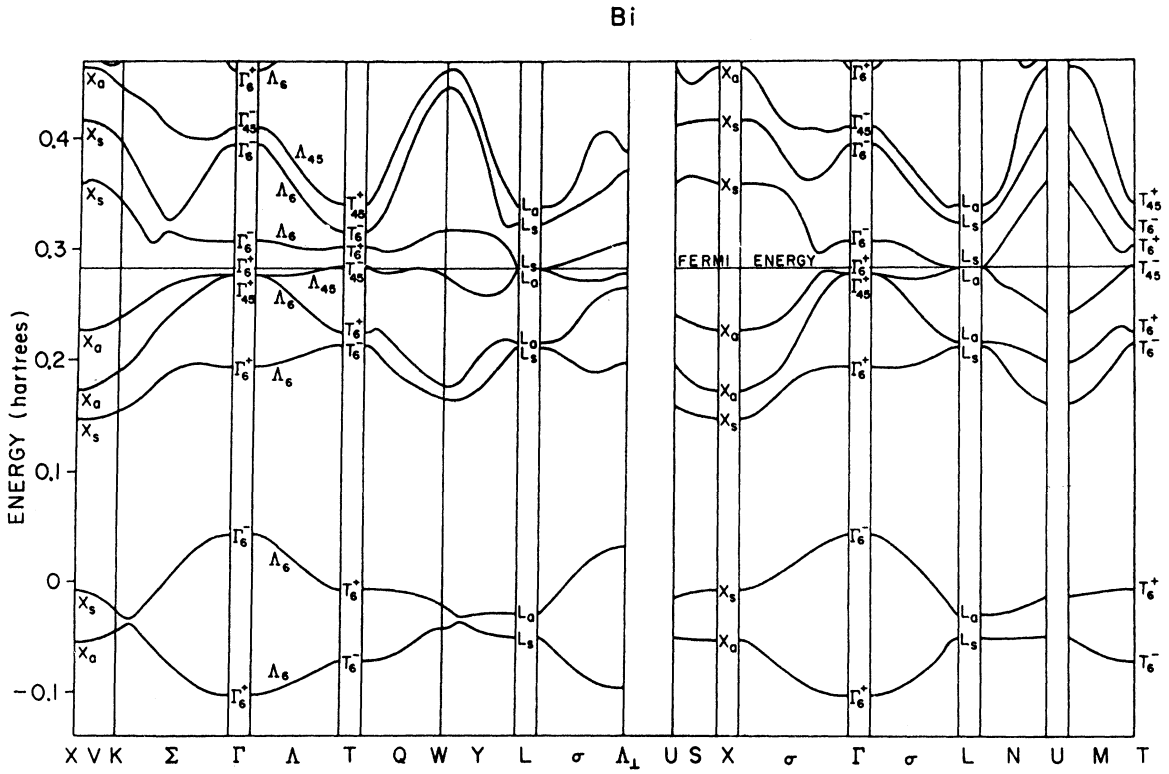

FIG. 1. The full-zone energy-band model for bismuth according to Golin (Ref. 1). The tightly coupled valence and conduction bands near the Fermi level are the L_a and L_s bands separated at the L point by an energy gap E_g.

the trigonal direction. Furthermore, this experiment is expected to provide a critical test for such departures since the magnetoreflection technique yields information on the energy bands over a wide range of energy and wave vector. The most significant result with regard to this aspect of the magnetoreflection study ($\vec{H} \parallel$ trigonal axis) is that no departures from the Lax two-band model are found over the entire range of magnetic fields and photon energies where interband Landau-level resonances are observed. This observation, along with the results obtained for $\vec{H} \parallel$ binary and bisectrix axes, leads to some interesting conclusions about the energy-band structure of bismuth in the vicinity of the L point, and these conclusions are discussed in Sec. III.

II. EXPERIMENTAL RESULTS

In our experiments, the optical reflectivity R of a liquid-helium-cooled single-crystal-bismuth sample is measured as a function of magnetic field H and photon energy $\hbar\omega$, using the Faraday geometry ($\vec{H} \parallel \vec{k}$ where $\vec{k}$ is the optical propagation vector). The principal features of the experimental apparatus have been described previously.[2,13] The improvement in the equipment that has been essential to the present work is the introduction of an Enhancetron signal averager to improve the signal-to-noise ratio. The effectiveness of this device can be seen in Fig. 2. Here the direct recorder trace displays the output of the detector amplifier and this trace is compared with the result of averaging together six such traces. This improvement in the signal-to-noise ratio provided more accurate observation of the magnetoreflection spectrum for the magnetic field H along the binary and bisectrix directions; this improvement, furthermore, made possible the observation of the spectrum for H along the trigonal direction, which had not been previously investigated.

The experimental trace of Fig. 2 was taken at a photon energy of $\hbar\omega = 0.0815$ eV, with the geometry $\vec{H} \parallel \vec{k}$, and $\vec{H}$ along the trigonal direction. As a first guess, the magnetoreflection spectrum observed from this cleaved trigonal face was analyzed in terms of the Lax two-band model,[4] which had been successful in the interpretation of previous magnetoreflection experiments.[2] In the present analysis, it was assumed that each peak in the reflectivity is associated with a resonance corresponding to an allowed interband Landau-level transition, and in Fig. 3 these resonances have been plotted as open circles and labeled in accordance with the notation of BML.[2] No $n = 0$ resonances were observed for $\vec{H} \parallel$ trigonal axis because these resonances presumably occur at $H \gg 100$ kG[15] for the range of available photon energies. In addition to the experimental data, the theoretical resonant fields and photon energies predicted by the Lax two-band model have been plotted as solid lines in Fig. 3. The band parameters for these curves were found by fitting the theory to the data, using an rms error minimizing technique. The results are summarized in Table I. As can be seen, the agreement between theory and experiment is excellent, and no effects associated with departures from the two-band model were

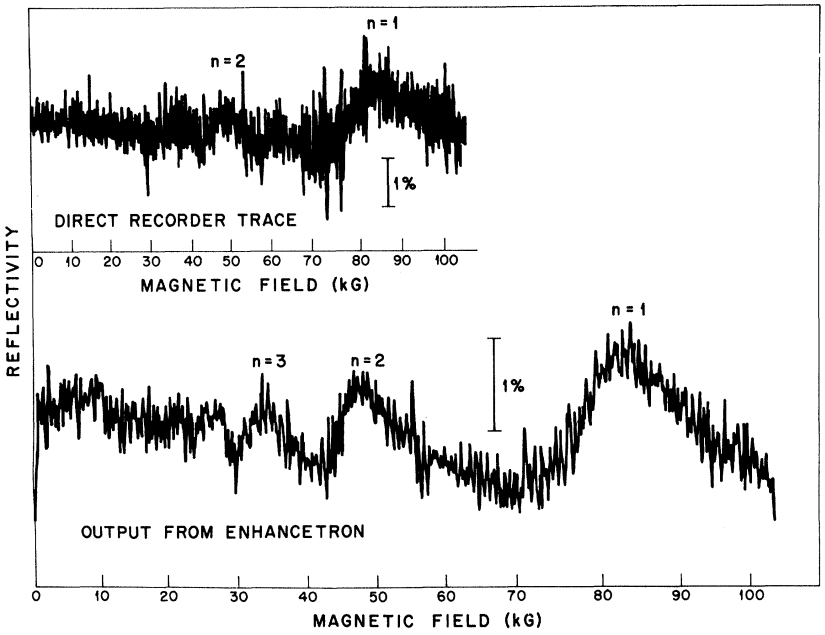

FIG. 2. Experimental magnetoreflection traces taken from a cleaved trigonal bismuth face with $\vec{H}$ in the trigonal direction. The photon energy is $\hbar\omega = 0.0815$ eV and the amplitude is expressed as a percentage of the zero field reflectivity. A comparison is made between the direct recorder trace and the enhancetron computer output after six traces.

TABLE I. Electronic band parameters for bismuth.

Parameter		Present work	BML [a]	SBR [b]
E_g in meV		11	15	15.3
β^* in meV/kG				
trigonal		1.25	···	0.82
binary	light	7.47	4.71	5.50
	heavy	···	···	0.42
bisectrix	light	8.44	5.47	6.36
	heavy	4.24	2.55	3.17
m_c^* at bottom of band				
trigonal		0.0093	···	0.0141
binary	light	0.00156	0.00246	0.00210
	heavy	···	···	0.0277
bisectrix	light	0.00137	0.00212	0.00182
	heavy	0.00273	0.00455	0.00364
$E_g m_c^*$ in eV [c]				
trigonal		1.2	···	1.1
binary	light	7.1	6.1	7.3
	heavy	···	···	0.55
bisectrix	light	8.0	7.1	8.4
	heavy	4.0	3.3	4.2

[a] Taken from magnetoreflection data of Brown, Mavroides, and Lax (Ref. 2).

[b] Taken from deHaas–Shubnikov data of Smith, Baraff, and Rowell (Ref. 9).

[c] m_c^* is taken at the band extremum.

found for $\vec{H}$ in the trigonal direction. In Sec. III, we discuss the significance of this unexpected result.

It should be pointed out here, however, that the magnetoreflection results are satisfied by an *ellipsoidal* two-band model. Although nonellipsoidal effects are expected to be most pronounced for this magnetic field orientation, [5] there seems no need to invoke nonellipsoidal complications to explain the magnetoreflection data.

The applicability of a two-band model was also tested with magnetoreflection measurements made with $\vec{H} \parallel$ binary and bisectrix axes, the sample orientations used by BML. [2] An experimental trace taken with $\vec{H} \parallel$ binary axis is shown in Fig. 4. For this photon energy of $\hbar\omega = 0.107$ eV, the $n = 0$ resonance occurs at $\vec{H} > 100$ kG, the maximum available field; since the reflectivity between 40 and 100 kG shows no structure for this photon-energy value, the figure was terminated at 40 kG. The resonances of this figure have a very large amplitude, primarily due to the small cyclotron effective mass which occurs for $\vec{H}$ in the binary direction (see Table I). The data taken with $\vec{H} \parallel$ binary axis essentially confirm the earlier results of the BML study [2] so that the significant conclusions that follow from the present work are (a) the peaks in the magnetoreflection spectrum display no observable fine structure (see Fig. 4) and (b) the Lax two-band model provides an excellent description of the observed magnetoreflection spectrum (see Fig. 5). Figure 5 gives a summary of the magnetoreflection resonances for $\vec{H} \parallel$ binary axis. These data cover a much larger range of magnetic fields and photon energies than the earlier work, [2] and are included here to demonstrate how well the two-band model (solid curves) follows the data (open circles). The fit to all the interband Landau-level transitions ($n = 0$ through $n = 7$) is made using two parameters, the effective cyclotron mass and the energy-band gap. Departures from the two-band model only begin to appear at the highest photon energies and magnetic fields. Here, changes in the line shape are also observed, indicating that at these large photon energies other bands are becoming important and the Lax model is beginning to break down. Using the band parameters determined from the interband Landau-level transitions (and no additional information), the dashed curve for the cyclotron resonance transition was computed; this curve agrees well with the cyclotron resonance measurements (shown as the open circles). For this magnetic-field orientation, the line shape observed in the low-photon-energy limit is essentially the same as that shown in Fig. 3(b) of BML. [2] The present cyclotron resonance results are in good agreement with the far-infrared measurements of Hebel and Wolff, [16] both with regard to line shape and resonant frequency. The agreement with regard to the resonant frequency is demonstrated by

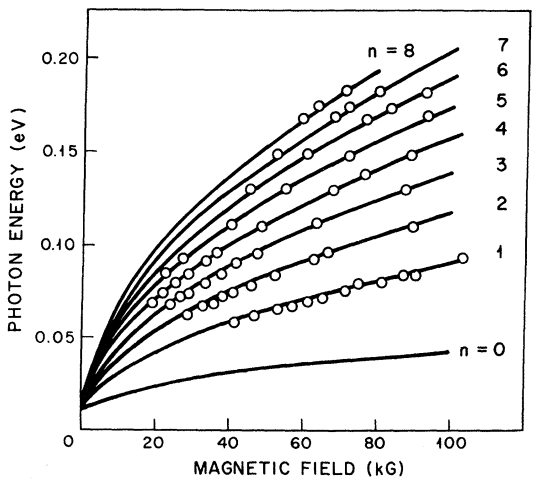

FIG. 3. Summary of the experimental (open circles) and theoretical (solid lines) values for the resonant magnetic fields and photon energies in the magnetoreflection spectrum from a trigonal bismuth face.

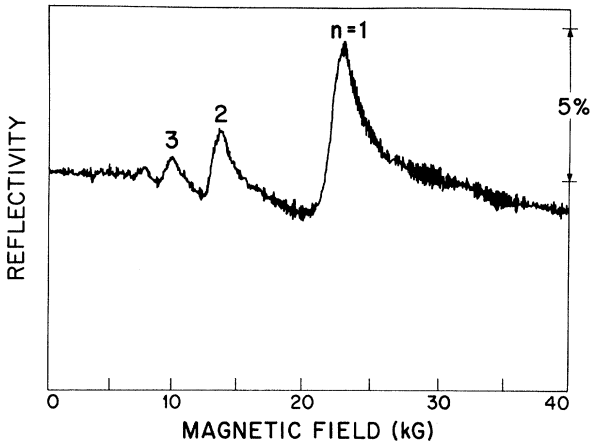

FIG. 4. Experimental magnetoreflection trace taken from a binary bismuth face and $\hbar\omega = 0.107$ eV. The resonances are labeled in accordance with the notation of Ref. 2.

the Hebel and Wolff point[16] given in Fig. 5. In constructing Fig. 5, the resonant fields for the interband Landau-level transitions were taken at the reflectivity maxima, while for the cyclotron resonance the steepest portion of the reflectivity rise was selected.[17]

For $\vec{H} \parallel$ bisectrix, a more complicated magnetoreflection spectrum is observed and the improved signal-to-noise ratio made possible a more systematic study of the spectrum for this sample orientation. Representative experimental traces for $\vec{H}$ in the bisectrix direction are shown in Figs. 6 and 7. Figure 6, which is more typical of the data in the higher photon-energy range, is similar to that of Fig. 8 in BML,[2] but differs in detail. The magnetoreflection spectrum shown in Fig. 6 is more complicated than that shown in Fig. 4, since, in the bisectrix case, relatively small cyclotron effective masses occur for both the principal and nonprincipal ellipsoids.[18] For the bisectrix magnetic field orientation, the electrons in the single principal ellipsoid have the smaller cyclotron effective mass and give rise to the series of interband Landau-level resonances for the "light" carriers, and these are denoted in Fig. 8 by the subscript l and by open circles. The carriers in the two equivalent nonprincipal ellipsoids have a heavier cyclotron effective mass and give rise to the more closely spaced resonances denoted by h and by closed circles in this figure. In contrast to this situation, the cyclotron effective mass for the principal ellipsoid for the magnetic field along a binary direction is so large that the interband Landau-level resonances have unobservably small amplitudes; thus, the resonances of Fig. 4 are associated with the two equivalent nonprincipal ellipsoids.[18]

The identification of the resonances associated with the heavy carriers in Fig. 6 was clarified to some extent by polarization experiments. With the optical electric field orientation $\vec{E} \parallel$ binary axis, the resonances associated with the heavy electrons are almost completely extinguished, whereas the light electron resonances are strong for both $\vec{E} \parallel$ binary axis and $\vec{E} \parallel$ trigonal axis. This polarization effect arises from the large anisotropy of the electron effective-mass tensor, which causes the bands associated with the various ellipsoids to couple differently to the two polarizations of $\vec{E}$. No striking polarization effects are observed in the magnetoreflection spectrum for $\vec{H}$ in the binary direction.

The magnetoreflection spectrum for $\vec{H}$ in the bisectrix direction was also studied in the limit of low photon energies, and a recorder trace characteristic of this limit is shown in Fig. 7. The spectrum here is seen to be quite different from that of Fig. 6, which is typical of the higher photon-energy range. The present work is the first de-

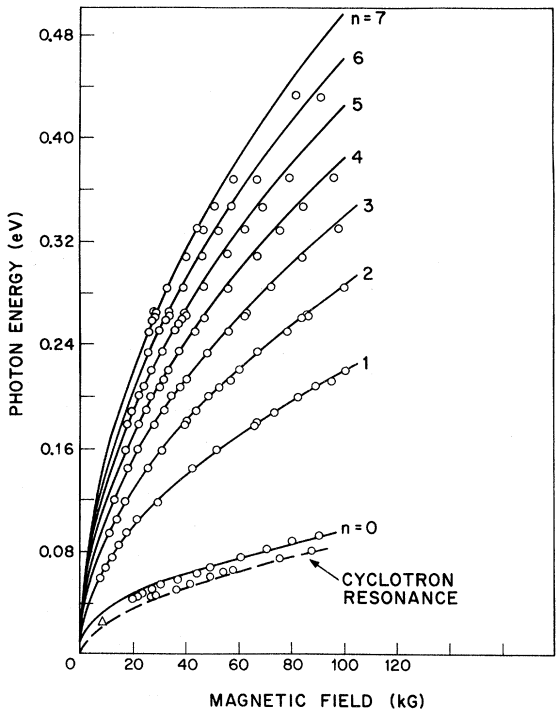

FIG. 5. Summary of the experimental (open circles) and theoretical (solid lines) values for the resonant magnetic fields and photon energies in the magnetoreflection spectrum from a binary bismuth face. Data for both interband Landau-level transitions and cylotron resonance are shown. The Δ point is taken from the cyclotron resonance data of Hebel and Wolff (Ref. 16).

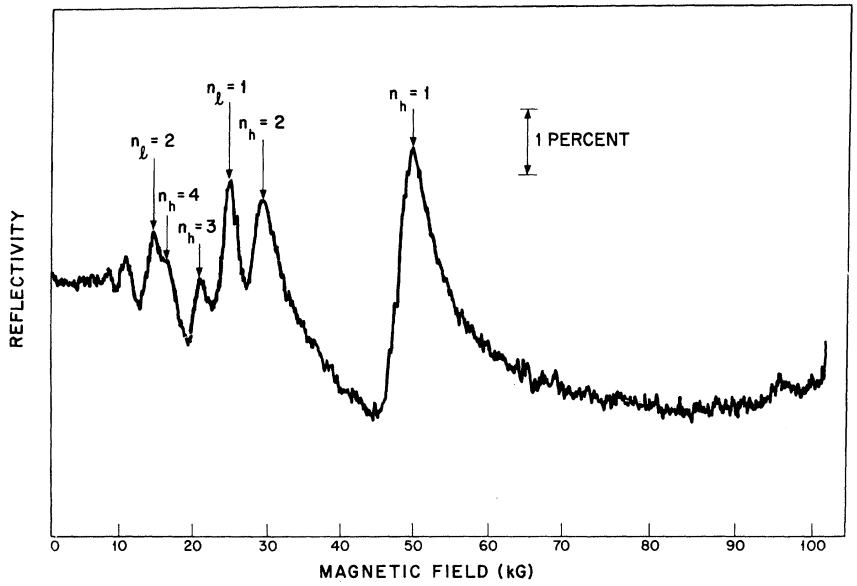

FIG. 6. Experimental magnetoreflection trace taken from a bisectrix bismuth face and $\hbar\omega = 0.1165$ eV using the enhancetron computer output for the average of four traces. The l and h subscripts refer, respectively, to the light and heavy cyclotron masses that occur in this orientation.

tailed study in this limit, where the improvement in signal-to-noise ratio provided by the Enhancetron computer is essential for the study of the spectrum. In Fig. 7, not only do the resonant fields of the $n = 0$ transitions depend strongly on the nonparabolic features of the two-band model, but the line shapes are also characteristically different from those of the higher quantum-number transitions. Also seen in this figure are the cyclotron resonance lines for the light- and heavy-mass electrons.

A summary of the observed interband and cyclotron resonance transitions for $\vec{H} \parallel$ bisectrix axis is given as the open circles in Fig. 8 and a fit to the interband data is made by the Lax two-band model in terms of two parameters, the energy-band gap E_g and the cyclotron effective mass m_c^* (see Table I for explicit values). From this figure it is seen that the two-band model accounts very well for the bisectrix magnetoreflection spectrum. Using the band parameters determined from the interband data, the two-band model also provides very good agreement with the observed cyclotron resonance transitions. Thus, the bisectrix magnetoreflection spectrum can be explained quantitatively by the Lax two-band model.[4] To put this another way, no fine structure is observed in this spectrum that cannot be handled by the two-band model, in contrast with the dHvA-type results.[8-11]

From both the binary and bisectrix data, the energy-band gap of the two-band model is determined to be $E_g = 11 \pm 1$ meV. A relatively accurate value for E_g is obtained in the present work because of the large amount of data taken in the low quantum limit. Since the magnetoreflection data for the $n = 0$ transition with $\vec{H} \parallel$ trigonal axis are not available, the energy-band gap cannot be accurately deduced from the trigonal magnetoreflection data. For this reason, the trigonal data were interpreted with the two-band model using only one adjustable parameter, the cyclotron effective mass, and constraining the energy gap to the 11-meV value as determined from the binary and bisectrix magnetoreflection data.

The most detailed determination of the effective-mass tensor and the cyclotron effective masses for the electrons in bismuth was made in the de Haas–Shubnikov studies of Smith, Baraff, and Rowell,[9] where the analysis was carried out using the Lax two-band model and a value of $E_g = 15.3$ meV. This value of E_g is close to the value of $E_g = 15$ meV reported by BML.[2] Because of the different values taken for E_g, discrepancies appear between the cyclotron effective masses m_c^* as determined by Smith, Baraff, and Rowell[9] and by the present magnetoreflection study (see Table I). The principal reason for this discrepancy is the form of the two-band model. In bismuth, both the de Haas–Shubnikov periods and the location of the magnetoreflection resonances depend primarily upon the quantity E_g/m_c^*; and if, instead of m_c^*, we compare values for E_g/m_c^*, then good agreement is obtained between the present magnetoreflection data and the de Haas–Shubnikov data.[9] This can be seen in Table I, where the results for E_g/m_c^* are also included. In comparing these experiments, it is of interest to observe that to within experimental error, there is no evidence for any difference in the cyclotron effective mass in bismuth as observed at high frequencies $\omega \gg \omega_q$ and at low frequencies $\omega \ll \omega_q$, where

ω_q is a measure of the optical-phonon frequency. The magnetoreflection experiment is carried out in the high-frequency limit, while the dHvA experiments take place in the low-frequency limit.

III. DISCUSSION

The experimental results summarized above indicate that the magnetoreflection experiment can be analyzed entirely within the framework of the Lax two-band model. On the other hand, the analysis of the dHvA-type experiments requires the introduction of other bands to remove the degeneracy of the Landau levels. It is the purpose of this section to show how these two results can be reconciled.

In this connection we will first present some of the previously developed theoretical treatments of the strongly coupled valence and conduction bands of bismuth. We will then use our experimental results to simplify this theory, and discuss the implication of this simplification.

The most general effective Hamiltonian $\mathcal{H}_B$ describing two strongly coupled nondegenerate (except for spin) bands in the vicinity of the L point in the Brillouin zone was developed by Baraff,[12] and may be written as

$$\mathcal{H}_B = \mathcal{H}_W + \mathcal{H}_p, \tag{7}$$

where $\mathcal{H}_W$ is the two-band Hamiltonian, extensively studied by Wolff,[6] and describes the interaction of the two strongly interacting bands with each other. The perturbation Hamiltonian $\mathcal{H}_p$ of Eq. (7) is assumed to be small compared with $\mathcal{H}_W$ and describes the interaction of the two strongly coupled bands with the other bands nearby. In the Lax two-band model, it is assumed that $\mathcal{H}_p$ is zero, and the Hamiltonian $\mathcal{H}_W$ is diagonalized in the presence of a magnetic field to yield the Landau-level energies of Eq. (1).

It is important to note that Eq. (1) yields doubly degenerate Landau levels, except for those with $j = 0$; here, we can only have $s = \frac{1}{2}$, since the $s = -\frac{1}{2}$ level does not exist. In the presentation which follows, we do not discuss these nondegenerate levels, since a consideration of this special case does not affect our conclusions in any way, but merely makes the presentation much more complicated.

Using $\mathcal{H}_W$, Wolff calculated the velocity matrix elements[6] for transitions between the Landau levels as a function of k_H, n, s, n', and s', where the orbital and spin quantum numbers n, s and n', s' correspond, respectively, to the initial and final states. He found that for arbitrary k_H these transitions were allowed only when $\Delta n = 0$, $\Delta s = \pm 1$, or $\Delta n = \pm 1$, $\Delta s = 0$. In addition, he found that only the spin-conserving ($\Delta s = 0$) transitions were allowed at $k_H = 0$, where the extremum in the joint density of states occurs. One might expect, therefore, that the contribution of the spin-flipping transitions to the dielectric constant would lead to much smaller structure in the magnetoreflectivity than the spin-conserving transitions. By calculating the dielectric constant of bismuth using the one-electron density matrix formalism, and the k_H-dependent Landau-level energies and velocity matrix elements as given by Wolff,[6] we have substantiated this assumption[13]; the observed resonances in the magnetoreflectivity of bismuth are found to be almost

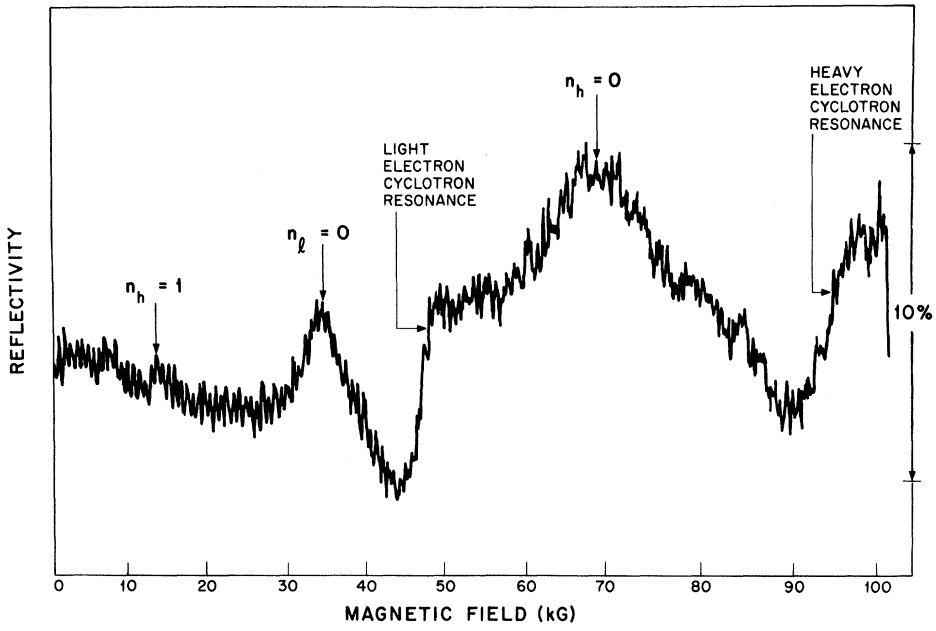

FIG. 7. Experimental magnetoreflection trace taken from a bisectrix bismuth face and $\hbar\omega = 0.0618$ eV using the enhancetron computer output for the average of two traces.

completely due to the spin-conserving transitions.[13]

Thus, every interband Landau-level resonant structure in the magnetoreflection spectrum as predicted by the Wolff selection rules[6] would consist of contributions from the four degenerate resonant transitions, which may be written $b, j, s \rightarrow -b, j+1, s$, where $s = \pm\frac{1}{2}$, and the band indices are $b = \pm 1$. Degenerate with these resonances are the unobservably small spin-flipping resonances, which may be written as $b, j, s = \frac{1}{2} \rightarrow -b, j+1, s = -\frac{1}{2}$, where again $b = \pm 1$. Both the spin-conserving and spin-flipping transitions are illustrated schematically in Fig. 9. The Wolff selection rules[19] apply to the Lax two-band model where $\mathcal{H}_p = 0$ and the energy levels depend only upon quantum number j. The resulting doubly degenerate energy levels are shown on the left-hand side of this figure.[20] This energy-level degeneracy leads to the sixfold degeneracy in the resonant photon energy corresponding to both spin-conserving transitions (fourfold) and the spin-flipping transitions (twofold).

In analyzing their data, BML[2] used Eq. (1) with $k_H = 0$ for the Landau-level energies and simplified the labeling by indexing each observed resonance with the orbital quantum number (n) of the two levels involved in the spin-flipping transition; ac-

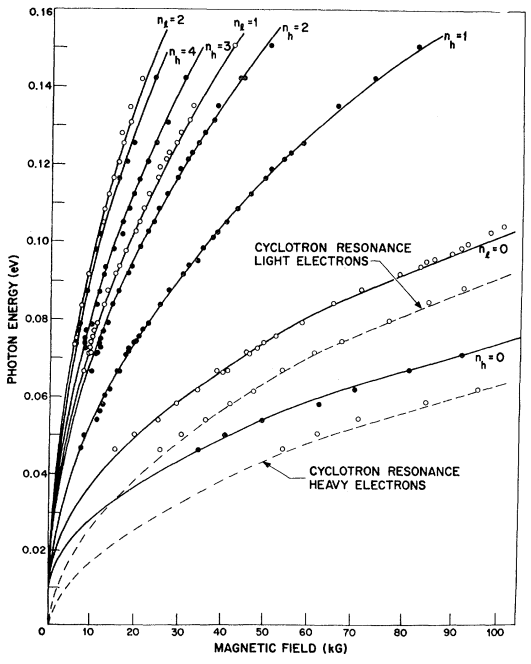

FIG. 8. Summary of the experimental and theoretical values for the resonant magnetic fields and photon energies in the magnetoreflection spectrum from a bisectrix bismuth face. For the interband Landau-level transitions, the light-mass data are given as the open circles and the heavy-mass data as the closed circles.

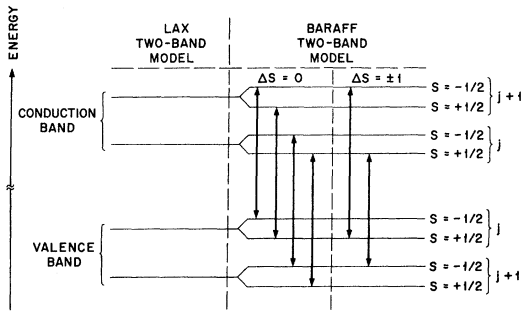

FIG. 9. Schematic representation of the allowed interband Landau-level transitions in bismuth according to the Lax and Baraff versions of the two-band model. The four spin-conserving and two spin-flipping transitions of the Baraff model become degenerate in energy for the Lax model.

cording to the Lax model, these energy differences are degenerate with the energy for the spin-conserving transitions which actually produce the observable resonances.

Although it is found that by using the above method of analysis an extremely good fit can be obtained to both the data of BML and the data reported in this paper, it is also clear from dHvA-type experiments[8-11] that the perturbation Hamiltonian $\mathcal{H}_p$, although small, produces observable effects. The fine structure in the dHvA data shows that the j, s and j, $-s$ Landau levels are not degenerate. In order to understand this splitting, Baraff,[12] using first-order perturbation theory, calculated the energy shifts which occur when the perturbation Hamiltonian is assumed to be nonzero. The Baraff Hamiltonian[12] allows the bands of the two-band model to interact with other bands not explicitly treated in the Wolff two-band Hamiltonian.[6] The Landau-level energies at $k_H = 0$ obtained in the Baraff treatment can be written as

$$E^B_{b,j,s} = E^0_{b,j} + f_+ + f_- , \tag{8}$$

where the perturbation terms f_+ and f_- depend on spin s, as well as on the band index b and the quantum number j, and are given by

$$f_\pm = [(E^0_{b,j} \pm \epsilon)/E^0_{b,j}](B_\pm j \pm G_\pm s)\beta^* H, \tag{9}$$

in which the orbital correction terms are described by

$$B\pm = \vec{H} \cdot \overleftrightarrow{A}_\pm \cdot \vec{H} / \vec{H} \cdot \overleftrightarrow{m}^* \cdot \vec{H} \tag{10}$$

and the spin correction terms by

$$G\pm = \vec{H} \circ \overleftrightarrow{F}_\pm \cdot \vec{H} / \vec{H} \cdot \overleftrightarrow{m}^* \cdot \vec{H} . \tag{11}$$

In these equations, the energy gap $E_g = 2\epsilon$, and the five tensors $\overleftrightarrow{m}^*$, $\overleftrightarrow{A}_\pm$, and $\overleftrightarrow{F}_\pm$ are to be experimentally determined.

In order to analyze the magnetoreflectivity data in terms of the more general Baraff Hamiltonian, we also need to find the selection rules for transitions between the eigenstates of $\mathcal{H}_B$. To determine these selection rules, we first note that the matrix elements of $\mathcal{H}_p$ between the degenerate b, j, s and b, j, $-s$ eigenstates of $\mathcal{H}_W$ vanish at $k_H = 0$. There is, therefore, no zeroth-order mixing of these two states at $k_H = 0$, where the singularity in the joint density of states occurs. Secondly, we note that $\mathcal{H}_p$ is quite small, as shown by the experimental dHvA data.[8-11] It therefore seems reasonable to assume that at $k_H = 0$ the velocity matrix elements for transitions between the Baraff states are very similar to the ones calculated by Wolff.[6] From our magnetoreflection line-shape calculation,[13] we have found that the selection rules are essentially determined by the velocity matrix elements at $k_H = 0$, where the extremum in the joint density of states occurs; therefore, it seems reasonable to assume that the selection rules calculated by Wolff[6] are still essentially correct.

In Fig. 9 we have, therefore, used these selection rules to draw the four spin-conserving and two spin-flipping interband Landau-level transitions for the Baraff model; we recall that according to the Lax two-band model, all six of these transitions are degenerate. If all the tensors in Eqs. (10) and (11) are independent of each other, it can easily be seen that none of these transitions are degenerate when the first-order perturbations, as described by Eqs. (8)–(11), are taken into account. Thus, the Baraff Hamiltonian predicts, in general, fine structure in the magnetoreflectivity spectrum. However, no such fine structure has been observed with the magnetic field along any of the principal crystalline axes. We have, therefore, made the simplest assumption consistent with the data; that is, we assume that all of the spin-conserving transitions in Fig. 9 are degenerate. This assumption has, in fact, been used in constructing Fig. 9. This restriction, however, requires that

$$\overleftrightarrow{A}_+ = -\overleftrightarrow{A}_- \equiv \overleftrightarrow{A}\ , \tag{12a}$$

$$\overleftrightarrow{F}_+ = -\overleftrightarrow{F}_- \equiv \overleftrightarrow{F}\ , \tag{12b}$$

so that

$$B_+ = -B_- \equiv B\ , \tag{12c}$$

$$G_+ = -G_- \equiv G\ . \tag{12d}$$

With these restrictions, we may now write the Baraff magnetic energy levels at $k_H = 0$ in the simpler form[21]

$$E^B_{b,j,s} = E^0_{b,j} + 2\beta^* H[(\epsilon/E^0_{b,j})Bj + Gs], \quad j \neq 0. \tag{13}$$

It can be seen that the spin degeneracy of these levels is lifted through the spin-splitting parameter G. Equation (13) can be even further simplified by defining a new effective-mass tensor

$$\overleftrightarrow{M}^* \equiv (\overleftrightarrow{m}^* + 4\overleftrightarrow{A})(\det\overleftrightarrow{m}^*)^{1/2}/[\det(\overleftrightarrow{m}^* + 4\overleftrightarrow{A})]^{1/2}\ , \tag{14}$$

and a new quantity

$$\beta^{**} \equiv \beta_0(\hat{h}\cdot\overleftrightarrow{M}^*\cdot\hat{h})^{1/2}/(\det\overleftrightarrow{M}^*)^{1/2} = \beta^*(1+4\hat{B})^{1/2}\ . \tag{15}$$

Expanding the square root to the same accuracy as was achieved in deriving Eq. (8) (first order in the small quantities B and G), we find

$$\beta^{**} = \beta^*(1+2B). \tag{16}$$

Furthermore, since it can be shown to first order in B that

$$(\epsilon^2 + 2\epsilon\beta^{**}Hj)^{1/2} = E^0_{b,j} + 2\beta^* H(\epsilon/E^0_{b,j})Bj, \tag{17}$$

we finally find that we may write the expression for the Landau-level energy $E^B_{b,j,s}$ as

$$E^B_{b,j,s} = E^{0'}_{b,j} + 2s\beta^{**}GH, \tag{18}$$

where we have ignored the small difference between β^* and β^{**} in writing the small term $2s\beta^{**}GH$ and have defined $E^{0'}_{b,j}$ as

$$E^{0'}_{b,j} = \pm(\epsilon^2 + 2\epsilon\beta^{**}Hj)^{1/2}\ . \tag{19}$$

It is important to note that, though Eq. (18) is very simple in form, it includes all the effects due to $\mathcal{H}_p$ to first order in perturbation theory. The first term of this equation ($E^{0'}_{b,j}$) has precisely the same form as the Lax two-band energy levels $E^0_{b,j}$. The only difference is in the interpretation of the band parameters $\overleftrightarrow{M}^*$ and $\overleftrightarrow{m}^*$. In both cases, the physical significance of the effective-mass tensors is that they describe the curvature of the conduction band at the band extremum. In the Lax two-band model, this curvature is assumed to be completely due to the interaction between the tightly coupled valence and conduction bands,[4] while in the more complete theory of Baraff[12] it is recognized that a portion of the curvature is due to the interaction of the valence and conduction bands with the other bands

nearby. The second term of Eq. (18) describes the lifting of the degeneracy of the two-band model by the interaction with the nearby bands to first order in perturbation theory.

It is now clear why the two-band model describes the magnetoreflectivity spectrum so well. Essentially, the interband transitions which yield large resonances in the reflectivity are spin-conserving ones, so that the second term of Eq. (18) drops out of the expressions relating the resonance fields with the photon energies. We, therefore, obtain expressions which are exactly of the same form as are generated by the Lax model. Equation (18) also helps us to understand why the two-band model works so well even with the magnetic field along the trigonal axis, where coupling to bands outside the two-band model are known to be important.[5] The analysis given here shows that $\mathcal{H}_p$ has no effect on the magnetoreflectivity spectrum to first order in $\mathcal{H}_p$.

Finally, it should be pointed out that the relationships between the Baraff band parameters found in this paper are not predicted by any symmetry arguments and may, therefore, be valid only as a first approximation. Higher-resolution magnetoreflection measurements may, in fact, show very small splittings of the resonant structure and may also show two additional broad sidebands due to the "nonresonant" spin-flipping transitions. Such experiments would provide valuable information on the effective g factor for the valence band at point L in the Brillouin zone.

The simplest way to understand the band parameter relations which describe the present data [see Eq. (12)] is to assume that all the bands in the vicinity of the Fermi level at point L are interrelated in some fashion. The simplest physical picture consistent with the data assumes that for each band at an energy E, interacting with the valence band, there is another band at energy $-E$ which interacts just as strongly with the conduction band. This physical picture is not the only possible one, however, and many other band structures could also yield the relationships between the Baraff parameters implied by the present magnetoreflection results.

ACKNOWLEDGMENTS

We would like to express our thanks to D. F. Kolesar for help in carrying out the measurements. We are also grateful to Dr. G. A. Baraff, Dr. G. Dresselhaus, Professor B. Lax, Dr. J. G. Mavroides, Professor G. W. Pratt, Jr., Dr. Y. Shapira, and Dr. P. A. Wolff for many stimulating discussions.

---

†This paper is based on a thesis submitted by one of the authors (M. M.) in partial fulfillment for the Ph. D. degree in the Electrical Engineering Department, Massachusetts Institute of Technology, 1968 (unpublished).

*Work supported in part by the Office of Naval Research under Contract No. Nonr-1841(72) by the Advanced Research Projects Agency under Contract No. SD-90, by the Department of the Air Force.

‡Visiting scientists, Francis Bitter National Magnet Laboratory, Massachusetts Institute of Technology, Cambridge, Mass., supported by the U.S. Air Force Office of Scientific Research.

§Present address: Xerox Corporation, Rochester, N. Y.

[1]W. S. Boyle and G. E. Smith, *Progress in Semiconductors* (Heywood, London, 1963), Vol. 7, p. 1. A full-zone energy-band model for bismuth has been given by S. Golin, Phys. Rev. 166, 643 (1968).

[2]R. N. Brown, J. G. Mavroides, and B. Lax, Phys. Rev. 129, 2055 (1963). This paper is hereafter referred to as BML.

[3]E. O. Kane, J. Phys. Chem. Solids 1, 249 (1957).

[4]B. Lax and J. G. Mavroides, *Solid State Physics*, edited by F. Seitz and D. Turnbull (Academic, New York, 1960), Vol. 11, p. 368.

[5]M. H. Cohen, Phys. Rev. 121, 287 (1961).

[6]P. A. Wolff, J. Phys. Chem. Solids 25, 1057 (1964).

[7]The zero of energy is here taken to be half-way between the valence and conduction bands.

[8]J. S. Dhillon and D. Shoenberg, Phil. Trans. Roy. Soc. London A248, 1, (1955); Y. Saito, J. Phys. Soc. Japan 18, 1845 (1963).

[9]G. E. Smith, G. A. Baraff, and J. M. Rowell, Phys. Rev. 135, A1118 (1964).

[10]J. E. Kunzler, F. S. L. Han, and W. S. Boyle, Phys. Rev. 128, 1084 (1962).

[11]Y. Sawada, E. Burstein, and L. Testardi, J. Phys. Soc. Japan Suppl. 21, 7 (1966).

[12]G. A. Baraff, Phys. Rev. 137, A842 (1965).

[13]M. Maltz, thesis, Massachusetts Institute of Technology, 1968 (unpublished).

[14]These simplifications can also be exploited in deriving the k_H dependence of the magnetic energy levels for the Baraff model (see Ref. 13).

[15]The maximum magnetic field used in this study was ~ 105 kG.

[16]L. C. Hebel and P. A. Wolff, Phys. Rev. Letters 11, 368 (1963).

[17]The selection of these resonant fields was suggested by the line-shape calculation for these processes in bismuth using a two-band model (see Ref. 13).

[18]For a binary optical face, the principal L point is defined defined as the one lying in the mirror plane, perpendicular to that binary axis which is normal to the optical face. The other two L points are designated as nonprincipal ones. An analogous definition is made for the bisectrix optical face.

[19]These selection rules apply to intraband transitions ($\Delta b = 0$, $b = 1$) as well as interband transitions ($b = -1 \rightarrow b = +1$) (see Ref. 6).

[20]Figure 9 is applicable only to Landau-level transitions involving energy levels for which $j > 0$. The corre-

sponding diagram for the special transitions involving the $j=0$ levels is immediately constructed from the Wolff selection rules given in Ref. 6.

[21]Because of the complexity of the Baraff Hamiltonian, the treatment in Ref. 12 is confined to $k_H=0$.

PHYSICAL REVIEW B VOLUME 2, NUMBER 8 15 OCTOBER 1970

Discrete Variational Method for the Energy-Band Problem with General Crystal Potentials*

D. E. Ellis†
Department of Physics, University of Florida, Gainesville, Florida 32601
and
Department of Physics, Northwestern University, Evanston, Illinois 60201
and
G. S. Painter‡
Quantum Theory Project, University of Florida, Gainesville, Florida 32601
(Received 1 May 1970)

A general variational method for efficiently calculating energy bands and charge densities in solids is presented; the method can be viewed as a weighted local-energy procedure or alternately as a numerical integration scheme. This rapidly convergent procedure circumvents many of the difficulties associated with the evaluation of matrix elements of the Hamiltonian in an arbitrary basis and treats the general nonspherical potential with no more complication than the usual "muffin-tin" approximation. Thus the band structure of ionic and covalent materials can be calculated with realistic crystal potentials. As an example, the method is applied to the one-electron model Hamiltonian with a nonspherical local potential, using a linear combination of atomic orbitals basis. Matrix elements of the Hamiltonian are evaluated directly without decomposition into atomic basis integrals; no "tight-binding" approximations are made. Detailed calculations are presented for the band structure and charge density of bcc lithium which demonstrate the feasibility of our method, and reveal the sensitivity of the energy bands to nonspherical and exchange components of the crystal potential. Various prescriptions for the construction of crystal potentials are considered, and convenient least-squares expansions are described. The extension of these methods to nonlocal potentials such as are encountered in the Hartree-Fock self-consistent-field procedure is discussed.

I. INTRODUCTION

The energy-band model for crystalline solids has proved to be very useful in describing optical, magnetic, and transport properties of a variety of materials. The success of this model depends essentially on the choice of potential in the one-electron effective Hamiltonian. This potential may be determined in many ways, including an empirical set of parameters, the superposition of model free-atom potentials, or by a self-consistent iterative procedure based on a many electron picture. Two interrelated problems which must be solved in applying the theory are (a) to find a crystal potential which adequately accounts for electron correlation and (b) to develop computational methods powerful enough to handle realistic potentials. The very great progress made in understanding the electronic structure of metals has been aided by the fact that the free-electron "$\rho^{1/3}$" local exchange and the "muffin-tin" spherical average potentials are rather good approximations to the crystal potential. Computational methods such as the augmented-plane-wave (APW), KKR, and Green's-function schemes[1-3] exploit this simple form of the potential. However, in some cases, particularly for nonmetals, the results have been found to be sensitive to nonspherical components of the potential and/or deviations from the simple exchange approximation.[4,5] In addition to studying these effects, it now appears important to investigate the consequences of adopting effective potentials, nonlocal as well as local, based on pseudopotential, Hartree-Fock, or more fundamental many-electron models.

The approximations which simplify the energy-band treatment of metals seem to be practically useless for most ionic and covalently bonded solids. The aspherical ion crystal fields and the covalent charge distributions are not well represented by a spherical average, and the exchange model is ques-